Kinetics of Ring Formation

E. Ben-Naim[1] and P. L. Krapivsky[2]

[1]*Theoretical Division and Center for Nonlinear Studies,*
Los Alamos National Laboratory, Los Alamos, New Mexico 87545
[2]*Department of Physics, Boston University, Boston, Massachusetts 02215*

We study reversible polymerization of rings. In this stochastic process, two monomers bond and as a consequence, two disjoint rings may merge into a compound ring, or, a single ring may split into two fragment rings. This aggregation-fragmentation process exhibits a percolation transition with a finite-ring phase in which all rings have microscopic length and a giant-ring phase where macroscopic rings account for a finite fraction of the entire mass. Interestingly, while the total mass of the giant rings is a deterministic quantity, their total number and their sizes are stochastic quantities. The size distribution of the macroscopic rings is universal, although the span of this distribution increases with time. Moreover, the average number of giant rings scales logarithmically with system size. We introduce a card-shuffling algorithm for efficient simulation of the ring formation process, and present numerical verification of the theoretical predictions.

I. INTRODUCTION

Percolation [1, 2] controls many natural processes from polymer gelation [3–5] and diffusion in porous media [6, 7], to the spread of forest fires [8, 9] or infectious diseases [10–12]. In the standard percolation picture, a system evolves from a state with many small, microscopic, clusters into a state with a *single*, macroscopic, system-spanning, cluster. This phase transition is continuous, and it is controlled by the total number of connections between elementary units in the system.

In this study, we show that restricting the structure of the clusters leads to a different percolation behavior where multiple macroscopic clusters coexist. Percolation with multiple giant clusters has been recently reported in theoretical studies [13, 14], and it is relevant to the production of colloidal micro-gels [15, 16].

Our starting point is the classic polymer gelation process introduced by Flory [3–5, 17, 18], a simplified model that is essentially the mean-field theory for percolation [1, 19–23]. In this polymerization process, a very large number of molecular units ("monomers") join irreversibly to form clusters ("polymers"). This process has a second order phase transition between a "sol" phase in which all polymers are finite to a "gel" phase in which a *single* gel containing a finite fraction of the monomers in the system emerges. With time, this gel grows and eventually, it engulfs the entire system.

In the Flory model, there is no limit on the number of bonds per monomer, and the resulting polymers may have very different structures. We modify the polymerization process so that all polymers have the same structure. In our version, all monomers have exactly two bonds, so that all polymers are rings. Rings occur in magnetized powders or beads [24–26] because due to magnetic interactions, linear chains are unstable with respect to formation of rings (Figure 1). As is the case for magnetic beads, we consider directed rings where the bonds have directionality (Figure 2). The results extend
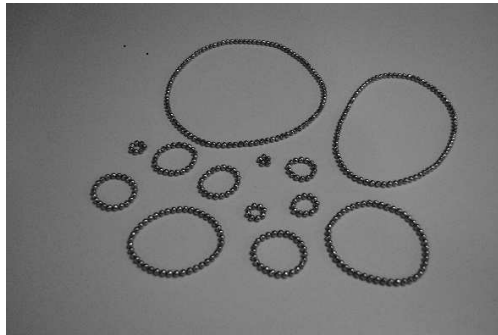

FIG. 1: Rings made of magnetic beads.

to undirected rings.

II. AGGREGATION-FRAGMENTATION PROCESS

At time $t = 0$, our system consists of N isolated monomers. These particles bond to form polymeric rings through the following process. In each elementary step, two monomers are selected at random and a first bond is drawn between them. Subsequently, both monomers drop an existing bond and then, the two "dangling" monomers form a second bond, as shown in Figure 2. Time is updated, $t \to t + \Delta t$ with $\Delta t = 2/N$, after each step so that each monomer experiences one bonding event per unit time. We note that the directionality of the first bond dictates the directionality of the second bond. This polymerization process conserves the total number of bonds because two bonds are gained and two bonds are lost in each event. We assign an imaginary self-bond to every original monomer, so that formally, the original monomers have a ring structure. Therefore, the total number of bonds in the system equals N. With this formulation, the polymerization process maintains a
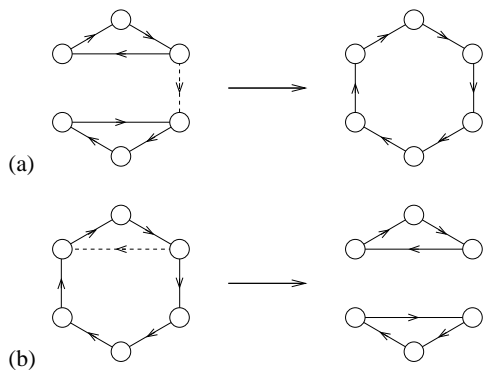
FIG. 2: (a) Inter-ring bonds lead to *aggregation*. (b) Intra-ring bonds result in *fragmentation.*

ring topology as every monomer has exactly two bonds.

The above polymerization process is equivalent to an aggregation-fragmentation process. When a monomer that belongs to ring of size i bonds with a monomer that belongs to a different ring of size j, a composite ring with size $i + j$ forms (Figure 2a). Hence, rings undergo the aggregation process

$$i, j \xrightarrow{K_{ij}} i + j \qquad \text{with} \qquad K_{ij} = ij. \qquad (1)$$

The aggregation rate K_{ij} is proportional to the product of the sizes because there are $i \times j$ distinct pairs that can bond. We note that the aggregation process (1) alone constitutes the Flory model.

A bond between two monomers in the same ring breaks that ring into two smaller rings. Schematically, the fragmentation process is (Figure 2b),

$$i + j \xrightarrow{F_{ij}} i, j \qquad \text{with} \qquad F_{ij} = \frac{i + j}{N}. \qquad (2)$$

Due to the circular symmetry, the fragmentation rate F_{ij} is proportional to the ring size, while the factor $1/N$ reflects that for fragmentation to occur, one must pick two monomers within the same ring. The fragmentation rate (2) is unusual as there is an explicit dependence on system size. Also, the aggregation-fragmentation process specified by (1) and (2) is reversible because for every aggregation event, there is an opposite fragmentation event, and vice verse.

Let $r_k(t)$ be the density of rings made of k monomers at time t. That is, if R_k is the expected number of rings of size k, then $r_k \equiv R_k/N$. This size density obeys the rate equation

$$\frac{dr_k}{dt} = \frac{1}{2} \sum_{i+j=k} ij\, r_i r_j - k r_k + \frac{1}{N} \left[\sum_{j>k} j r_j - \frac{k(k-1)}{2} r_k \right]. \quad (3)$$

The first two terms represent gain and loss due to the aggregation process (1), and the last two terms represent gain and loss due to the fragmentation process (2). In

particular, let us consider the two loss terms. The total aggregation rate is, by definition, the ring size k, but the total fragmentation rate, $F_k \equiv \sum_{i+j=k} F_{ij}$, grows quadratically with size, $F_k = \frac{1}{N} \binom{k}{2} = \frac{k(k-1)}{2N}$. Our goal is to understand the time evolution of the density $r_k(t)$, starting from the monomer-only initial condition, $r_k(0) = \delta_{k,0}$.

III. FINITE RINGS

Our implicit assumption is that the system is very large. When $N \to \infty$, one can use perturbation theory with the inverse system size being the small parameter [27]. We expand the size distribution to first order, $r_k = c_k + \frac{1}{N} g_k + \cdots$, and substitute this form into (3) to obtain the rate equation

$$\frac{dc_k}{dt} = \frac{1}{2} \sum_{i+j=k} ij c_i c_j - k c_k. \qquad (4)$$

The initial condition is $c_k(0) = \delta_{k,1}$. The two terms in this equation describe gain and loss due to aggregation. To zeroth order, the fragmentation process is negligible because the likelihood of picking two monomers within the same ring vanishes when $N \to \infty$. Equations (4) describe the evolution of the size distribution in the Flory model, where there is no fragmentation. The solution to these equations is well-known (see [20, 28] for a review)

$$c_k(t) = \frac{1}{k \cdot k!} (kt)^{k-1} e^{-kt}. \qquad (5)$$

Let $M_n(t) = \sum_{k \geq 1} k^n c_k(t)$ be the nth moment of the distribution c_k. The second moment diverges at a finite time as $M_2(t) = (1 - t)^{-1}$ for $t < 1$, a signature of the percolation transition at time $t = 1$. The first moment, $M_1(t)$, provides additional information about this phase transition. Consider the "missing mass" $g(t) = 1 - M_1(t)$. This quantity obeys the transcendental equation

$$g = 1 - e^{-gt}. \qquad (6)$$

When $t < 1$, there is only the trivial solution $g = 0$, and hence, finite clusters contain all of the mass. However, when $t > 1$, there is a second, nontrivial solution, $0 < g < 1$, and this solution is the physical one. Finite rings account for only a finite fraction, $M_1 = 1 - g$, of the total mass. Therefore, giant rings must account for the remaining fraction of the total mass, g. At time $t > 1$, the total mass of the giant rings equals $g(t)N$.

At time $t = 1$, the critical size distribution has a power-law tail (Figure 3),

$$c_k(1) \simeq \frac{1}{\sqrt{2\pi}} k^{-5/2}, \qquad (7)$$

when $k \gg 1$. At the critical point, the size of largest ring scales as $N^{2/3}$ with system size N [29–31].
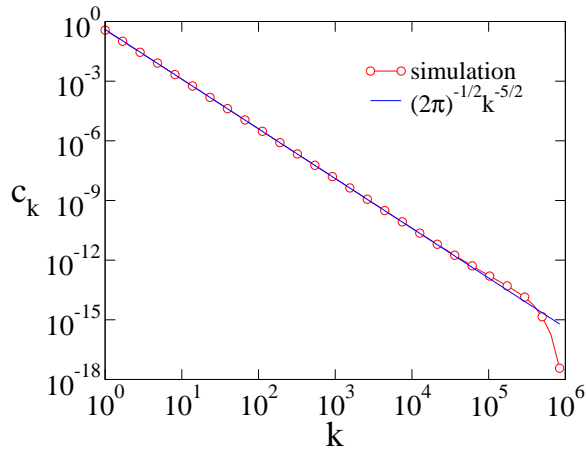
FIG. 3: (color online) The critical size distribution, $c_k \equiv c_k(t = 1)$ versus k. The simulation results are from 10^4 independent realizations of a system with $N = 10^8$.

IV. GIANT RINGS

When $t > 1$, we expect that macroscopic rings, that is, rings that contain a finite fraction of the total mass in the system, account for the missing mass. For a giant ring with size $k \propto N$, the total aggregation rate, k, and the total fragmentation rate, $\frac{k(k-1)}{2N}$, are both proportional to N. Hence, aggregation and fragmentation occur with comparable rates. Also, since both rates are proportional to the system size, aggregation and fragmentation are very rapid. To find the size distribution of the giant rings, we must consider the aggregation-fragmentation process governing the giant rings.

We characterize a giant ring using the normalized size, ℓ, defined as $\ell = k/N$. This quantity equals the fraction of the total mass contained in the ring. Let $G(\ell, t)$ be the average number of rings with normalized size ℓ at time t. Conservation of mass dictates

$$g(t) = \int d\ell\, \ell\, G(\ell, t), \qquad (8)$$

where $g(t)$ is the nontrivial solution of (6).

The quantity $G(\ell, t)$ satisfies

$$
\begin{aligned}
\frac{1}{N}\frac{\partial G(\ell, t)}{\partial t} &= \frac{1}{2}\int_0^\ell ds\, s(\ell - s)G(s, t)G(\ell - s, t) \\
&\quad - \ell(g - \ell)G(\ell, t) \\
&\quad + \int_\ell^g ds\, s\, G(s, t) - \frac{1}{2}\ell^2 G(\ell, t). \qquad (9)
\end{aligned}
$$

This rate equation, essentially the continuous analog of Eq. (3), describes the aggregation-fragmentation process that governs the giant rings. To formally derive (9) from (3), we first make the transformations $G_k \equiv Nr_k$ and $k = \ell N$, and then, note that the aggregation loss rate is reduced by the factor $(g - \ell)$ because self-interactions do not lead to aggregation.
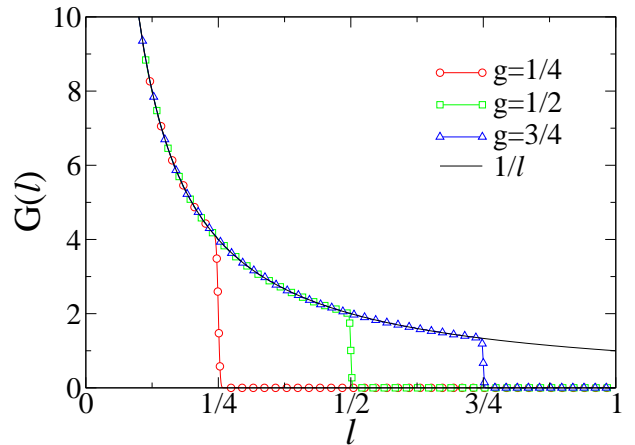

FIG. 4: (color online) Simulation results for $G(\ell) \equiv G(\ell, t)$ at three different times, $t(g = 1/4) = 1.150729$, $t(g = 1/2) = 1.386294$, and $t(g = 3/4) = 1.848392$. The time $t(g) = \frac{1}{g}\ln\frac{1}{1-g}$ follows from (6). Also shown for reference is the theoretical prediction (10). The simulations results are from 10^7 independent realizations of a system with size $N = 10^6$.

From the definition of $G(\ell, t)$ and from equation (8), we deduce that the quantity $G(\ell, t)$ is finite when $t > 1$ and $0 < g(t) < 1$. Therefore, the right-hand side of (9) is finite, while the left-hand side is negligible in the large-N limit. We therefore replace the left-hand side of Eq. (9) with zero to determine the *time-dependent* distribution $G(\ell, t)$. The resulting non-linear integral equation has the remarkably simple solution (see Figure 4)

$$
G(\ell, t) = \begin{cases} \ell^{-1} & \ell < g(t), \\ 0 & \ell > g(t). \end{cases} \qquad (10)
$$

Indeed, this solution obeys the mass conservation statement (8). Surprisingly, the size distribution is universal, although the span of the distribution grows with time, $0 < \ell < g(t)$. Therefore, at time $t > 1$, there are giant rings of all sizes up to the maximal value $g(t)N$.

The distribution of rings includes two distinct components: Nc_k gives the average number of finite rings, and $G(\ell)$ gives the average number of giant rings. Of course, the former expression applies at all times, while the latter holds only for $t > 1$. The giant rings grow at the expense of the finite rings and essentially they take over the entire system as $g \to 1$ when $t \to \infty$.

Finite rings and giant rings undergo separate, essentially decoupled, aggregation-fragmentation processes. Indeed, the rate equation (4) for c_k is closed, while the rate equation (9) for $G(\ell)$ is, in practice, also a closed equation. There is a constant flux of mass, $N \times dg/dt$, from finite rings to giant rings, and this flux couples the two types of rings. This coupling enters only through the fraction $g(t)$ which appears explicitly in (9).

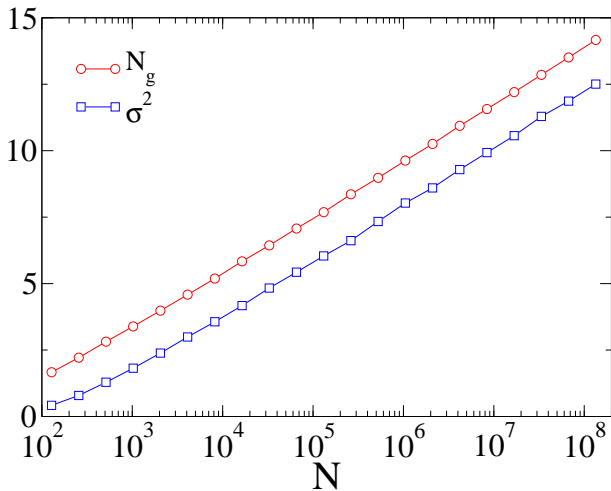The distribution (10) implies that there are multiple giant rings: the average number of giant rings, N_g, scales

FIG. 5: (color online) The average number of giant rings, N_g, and the variance σ^2, versus system size N. The simulation results represent an average over 10^5 independent realizations. We measured N_g and σ^2 by counting the number of rings with size $k > 4 \ln N$ at time $t = 2$.

FIG. 6: (color online) The largest three rings. Shown is the time evolution of $\ell_n(t)$, the size of the nth largest ring at time t, for $n = 1$ (upper red line), $n = 2$ (middle green line), and $n = 3$ (lower blue line). The results are from a single run of a system with $N = 10^6$. Also shown is the cumulative mass $g(t)$.

logarithmically with system size (Figure 5)

$$N_g \simeq \ln N. \qquad (11)$$

This behavior follows from $N_g = \int_{l_*}^{g} d\ell \, G(\ell)$. The lower limit $\ell_* = k_*/N$ can be deduced from the criterion $N \sum_{k \geq k_*} c_k(t) = 1$ that estimates the size of the largest *finite* ring. Using this criterion together with Eq. (5) we find $k_* \simeq (t - \ln t - 1)^{-1} \ln N$ and therefore $\ell_* \sim N^{-1} \ln N$.

Since the merger-breakup process is random, we expect that the variance in the number of giant rings, σ^2, is proportional to the mean, $\sigma^2 \simeq \ln N$. Numerical simulations confirm this behavior (Figure 5). Hence, the standard deviation

$$\sigma \simeq \sqrt{\ln N} \qquad (12)$$

quantifies fluctuations in the number of giant rings.

Figure 6 shows the normalized sizes of the three largest rings as a function of time using a simulated system. These sizes exhibit huge fluctuations as giant rings constantly merge and break on a very fast time scale. Interestingly, while the size of an individual giant ring is a stochastic quantity, the total size of all giant rings, $g(t)$, is a deterministic quantity.

The number of finite rings is proportional to N, while the number of giant rings scales only logarithmically with N. Equation (5) shows that monomers dominate in the long-time limit. By comparing the average number of monomers, $Nc_1 = Ne^{-t}$, with the the average number of giant rings, given by (11), we conclude that giant rings overtake finite rings when $t \gg t_f$ with
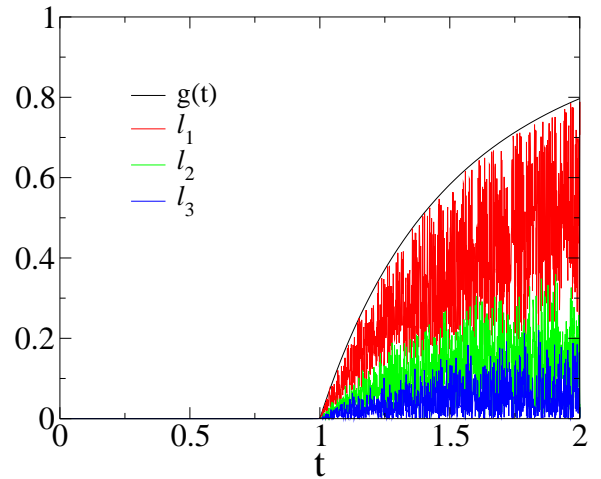
$$t_f \simeq \ln N. \qquad (13)$$

In writing this expression, we ignored secondary logarithmic corrections.

For times $t \gg t_f$, the ring-size distribution reaches a steady state. Setting $g = 1$ in (10) shows that N_k, the average number of rings with (unnormalized) size k, has the following form

$$N_k = \frac{1}{k}, \qquad (14)$$

for all $1 \leq k \leq N$. Thus, at the steady state, there are rings of all lengths, from finite rings to macroscopic rings. The distribution (14) also follows from the detailed-balance condition $K_{ij} c_i c_j = F_{ij} c_{i+j}$ with the solution $c_k = (Nk)^{-1}$ [28, 32].

In the steady state, aggregation generates an upward flux from small sizes to larger sizes, while fragmentation leads to a downward flux from large sizes to smaller sizes. These two fluxes perfectly balance. While the steady state distribution (14) includes rings of all sizes, rings of finite size account only for a microscopic mass, while rings of giant size account for nearly all of the (macroscopic) mass.

V. SHUFFLING ALGORITHM

Throughout this paper, we presented results of Monte Carlo simulations that support the theoretical predictions. We implemented an elegant algorithm that takes advantage of an isomorphism between the polymerization process and a card shuffling process. In the card shuffling algorithm [33–36], we start with an ordered deck of N cards, numbered 1 through N. Then, at each elementary step, we pick two cards at random and exchange their
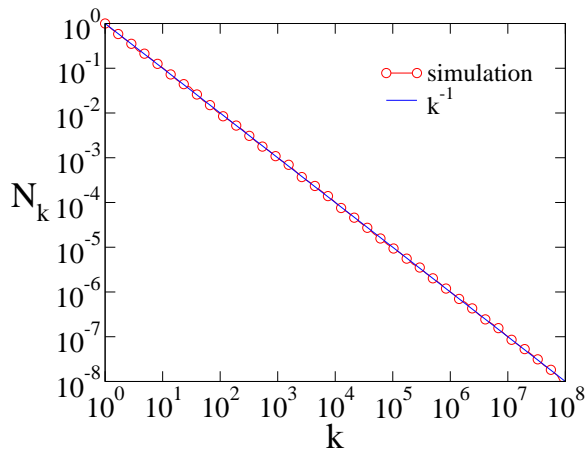
FIG. 7: (color online) The average number N_k of rings of size k at the steady state. The simulation results are from 10^3 independent realizations of a system with $N = 10^8$ at time $t = 20$.

positions. For example, the first two steps in shuffling a deck of 6 cards may look like

$$1\underline{2}3\underline{4}5\underline{6} \to 15\underline{3}4\underline{2}6 \to 154326 \to \cdots.$$

Time is updated by $\Delta t = 2/N$ after each step, $t \to t + 2/N$, and thus, each card participates in one shuffling event per unit time, on average.

We now use cycles to represent permutations. For example, six cards ordered 134265 are represented by (1)(234)(56) because there are three cycles: the card 1 forms a cycle of length one, the cards 234 form a cycle of length three, and the cards 56 form a cycle of length two. Initially, there are N cycles of length 1. Then, exchange of two cards in distinct cycles leads to merger, while exchange of two cards in the same cycle leads to breakup. For example, the following steps generate the merger and breakup events in Figure 2,

$$(1\underline{2}3)(4\underline{5}6) \to (156423), \quad \text{and} \quad (1\underline{5}64\underline{2}3) \to (123)(456).$$

Furthermore, the merger rate and the breakup rate are given by (1) and (2). Hence, the dynamics of cycles in the shuffling process are identical to the dynamics of rings in the polymerization process.

The above algorithm is straightforward and efficient. The shuffling steps take $\mathcal{O}(N)$ operations per unit time, and moreover, tracing the cycle structure requires only $\mathcal{O}(N)$ operations. This linear algorithm enabled us to simulate large systems with as many as $N = 10^8$. Figure 7 demonstrates the excellent agreement between the simulation results and the theoretical prediction (14).

The distribution N_k given in (14) equals the average number of cycles of length k for a random permutation of N elements [37, 38]. As expected, repeated shuffling randomizes the card order and according to (13), the number of exchanges required to generate a perfectly random shuffle scales as $N \ln N$.

A natural generalization is to n-card shuffling where n randomly chosen cards are reordered according to a prescribed rule. For example, if $n = 3$, we may follow the cyclic rule $123 \to 231$. The equivalent polymerization process now involves merger of n polymers. Straightforward generalization of the Flory model shows that the total gel mass, $g(t)$, satisfies [39]

$$1 - g = e^{-\frac{1-(1-g)^{n-1}}{(n-1)!}t}, \tag{15}$$

with $0 < g < 1$ in the giant-ring phase $t > (n-2)!$. We anticipate that the distribution of giant rings is given by (10), except that the total mass is now specified by (15). Our numerical simulations of the three-card process confirm this behavior.

VI. DISCUSSION

In summary, we studied a ring polymerization process in which a bond between two monomers results either in aggregation of two rings into one or in fragmentation of one ring into two. This process exhibits a percolation transition with a finite-ring phase in which all rings are microscopic and a giant-ring phase in which multiple macroscopic rings coexist. While the cumulative mass of the giant rings is deterministic, the sizes of individual giant rings are stochastic. Moreover, the giant rings exhibit huge fluctuations due to the extremely rapid merger and breakup processes. Finally, the size distribution of giant rings is stationary, although the span of this distribution grows with time.

The aggregation-fragmentation process that governs the rings is perfectly *reversible*. On the one hand, the distribution of ring size reaches a stationary state where detailed balance is formally satisfied. On the other hand, this final distribution is not thermodynamic because the number of rings varies logarithmically, rather than linearly, with system size. Phase transitions with non-thermodynamic states were previously observed only in *irreversible* aggregation-fragmentation processes [40–42].

The original Flory model is equivalent to an evolving random graph [17, 18, 22, 23, 28–31] in which a node can have an arbitrary degree. The ring formation process above generates an evolving regular random graph in which all nodes have degree 2. In this context, the fragmentation process illustrated in figure 2b naturally represents redirection of links. Hence, our analysis also constitutes the kinetic theory of an evolving regular random graph.

The ring formation process can be generalized in many ways. We focused on the mean-field version, and it will be interesting to study two-dimensional rings where spatial correlations play an important role. Another direction for further study is percolation of polymers with other types of fixed structures, for example, polymers where all monomers have exactly three bonds [3].

Finally, we notice that the unusual behaviors in the giant-ring phase are the consequence of the basic topological constraint, namely that the polymers maintain a ring structure. This suggests to investigate the influence of other constraints such as planarity [43, 44]. Another interesting question is what happens if the polymers are membranes [45] such as spheres (say due to the surface tension) that can merge and divide.

[1] D. Stauffer and A. Aharony, *Introduction to Percolation Theory* (Taylor & Francis, London, 1992).
[2] G. Grimmett, *Percolation* (Springer, Berlin, 1999).
[3] P. J. Flory, J. Amer. Chem. Soc. **63**, 3083 (1941).
[4] W. H. Stockmayer, J. Chem. Phys. **11**, 45 (1943).
[5] P. J. Flory, *Principles of Polymer Chemistry* (Cornell University Press, Ithaca, 1953).
[6] A. Bunde and S. Havlin (editors), *Percolation and Disordered Systems: Theory and Applications*, Physica A **366**, (1998).
[7] M. Sahimi, *Flow and Transport in Porous Media and Fractured Rock* (VCH, Boston, 1995).
[8] P. Bak, C. Tang, and K. Wiesenfeld, Phys. Rev. Lett. **59**, 381 (1987).
[9] B. Drossel and F. Schwabel, Phys. Rev. Lett. **69**, 1629 (1992).
[10] P. Grassberger, Math. Biosci. **63**, 157 (1983).
[11] M. E. J. Newman, Phys. Rev. E **66**, 016128 (2002).
[12] T. Tome and R. M. Ziff, Phys. Rev. E **82**, 051921 (2010).
[13] E. Ben-Naim and P. L. Krapivsky, J. Phys. A **38**, L417 (2005); J. Phys. Cond. Matter. **17**, S4249 (2005).
[14] W. Chen and R. M. D'Souza, arxiv:1011.5854.
[15] M. J. Murray and M. J. Snowden, Adv. Coll. Int. Sci. **54**, 73 (1995).
[16] B. R. Saunders and B. Vincent, Adv. Coll. Int. Sci. **80**, 1 (1999).
[17] R. Solomonoff and A. Rapaport, Bull. Math. Biophys. **13**, 107 (1959).
[18] P. Erdős and A. Rényi, Publ. Math. Inst. Hungar. Acad. Sci. **5**, 17 (1960).
[19] R. M. Ziff, E. M. Hendriks, and M. H. Ernst, Phys. Rev. Lett. **49**, 593 (1982).
[20] F. Leyvraz, Phys. Rep. **383**, 95 (2003).
[21] A. A. Lushnikov, Phys. Rev. Lett. **93**, 198302 (2004).
[22] S. Janson, T. Łuczak and A. Rucinski, *Random Graphs* (John Wiley & Sons, New York, 2000).
[23] B. Bollobás, *Random Graphs* (Academic Press, London, 1985).
[24] F. Kun, W. Wen, W. K. Pál, and K. N. Tu, Phys. Rev. E **64**, 061503 (2001).
[25] I. Varga, H. Yamada, F. Kun, H. -G. Matuttis, and N. Ito, Phys. Rev. E **71**, 051405 (2005).
[26] K. Kohlstedt, A. Snezhko, M. V. Sapozhnikov, I. S. Aranson, J. S. Olafson, and E. Ben-Naim, Phys. Rev. Lett. **95**, 068001 (2005).
[27] E. Ben-Naim and P. L. Krapivsky, J. Phys. A **37**, L189 (2004).
[28] P. L. Krapivsky, S. Redner and E. Ben-Naim, *A Kinetic View of Statistical Physics* (Cambridge University Press, Cambridge, 2010)
[29] S. Janson, D. E. Knuth, T. Łuczak, and B. Pittel, Rand. Struct. Alg. **3**, 233 (1993).
[30] B. Bollobás, C. Borgs, J. T. Chayes, J. H. Kim, and D. B. Wilson, Rand. Struct. Alg. **18**, 201 (2001).
[31] E. Ben-Naim and P. L. Krapivsky, Phys. Rev. E **71**, 026129 (2005).
[32] D. A. Lowe and L. Thorlacius, Phys. Rev. D **51**, 665 (1995).
[33] S. W. Golomb, SIAM Rev. **4**, 293 (1961).
[34] L. Flatto, A. Odlyzko, and D. Wales, Ann. Prob. **13**, 151 (1985).
[35] P. Diaconis and D. Aldous, Amer. Math. Month. **93**, 333 (1986).
[36] P. Diaconis, Proc. Natl. Acad. Sci. USA **93**, 1659 (1996).
[37] D. E. Knuth, *The Art of Computer Programming, vol. 3: Sorting and Searching* (Addison-Wesley, New York, 1998).
[38] M. Bóna, *Combinatorics of Permutations* (Chapman and Hall, Boca Raton, 2004).
[39] J. Jiang and H. Gang, Phys. Rev. B **39**, 4659 (1989).
[40] P. L. Krapivsky and S. Redner, Phys. Rev. E **54**, 3553 (1996).
[41] S. N. Majumdar, S. Krishnamurthy, and M. Barma, Phys. Rev. Lett. **81**, 3691 (1998).
[42] E. Ben-Naim and P. L. Krapivsky, Phys. Rev. E **77**, 061132 (2008).
[43] C. Godrèche, I. Kostov, and I. Yekutieli, Phys. Rev. Lett. **69**, 2674 (1992).
[44] P. Collet and J.-P. Eckmann, J. Stat. Phys. **121**, 1073 (2005).
[45] *Statistical Mechanics of Membranes and Interfaces*, ed. D. R. Nelson, T. Piran and S. Weinberg (World Scientific, Singapore, 1989).